

## Investigation of Relationship between the Response and Fourier Spectral Ratios Based on Statistical Analyses of Strong-Motion Records

Haizhong Zhang and Yan-Gang Zhao\*

*Department of Architecture, Kanagawa University  
3-27-1 Rokkakubashi, Kanagawa-ku Yokohama-shi  
Kanagawa 221-8686, Japan  
\*zhao@kanagawa-u.ac.jp*

Received 26 June 2020

Accepted 6 September 2020

Published 24 November 2020

In both seismic design and probabilistic seismic-hazard analyses, site effects are typically characterized as the ratio of the response spectral ordinate on the ground surface to that on the bedrock based on the scaling law borrowed from the Fourier spectral ordinate. Recent studies have shown that different from the Fourier spectral ratio (FSR), the response spectral ratio (RSR) does not purely reflect the site effects but also depends on the earthquake scenario even for linear analysis. However, previous studies are limited to theoretical analysis. This study statistically compares the two spectral ratios by analyzing many actual seismic ground motions recorded at nearby soil and rock sites. It is observed that the average RSR and FSR have similar overall shapes, and their maximum values occur at approximately the same period; however, the values around the peak are clearly different with FSRs consistently exceeding the RSRs. The RSR–FSR relationship depends on the earthquake scenario and the oscillator damping; their difference at periods longer than the site's fundamental period decreases as the magnitude and epicentral distance increase, and the RSRs generally approach the FSRs as the oscillator damping decreases.

*Keywords:* Response spectral ratio; Fourier spectral ratio; site effects.

### 1. Introduction

In both seismic design and probabilistic seismic-hazard analyses, the response spectral ordinate at a particular level of damping is always used to measure the ground-motion intensity [Li *et al.*, 2010]. In the construction of ground-surface response spectral ordinates, site effects are typically characterized as the ratio of the response spectral ordinate on the ground surface to that on the bedrock based on the scaling law borrowed from the Fourier spectral ordinate [Ibrahim *et al.*, 2014]. This means that the response spectral ratio (RSR) is assumed to purely represent the

\*Corresponding author.

effect of site conditions and be independent of the earthquake scenario for linear analysis. This assumption is widely adopted in ground-motion prediction models as well as seismic codes [Borcherdt, 1994; Dobry *et al.*, 2000; International Conference of Building Officials, 1997; ICC, 2012]. In the Japanese Seismic Design Code [Ministry of Land, Infrastructure and Transport, 2000], the RSR model is constructed even by considering the RSR to be identical to the Fourier spectral ratio (FSR) [Miura *et al.*, 2001; Midorikawa *et al.*, 2003; Zhang *et al.*, 2017; Zhang and Zhao, 2018, 2019]. However, Zhao *et al.* [2009]; Zhao and Zhang [2010] found that in contrast to the FSR, RSR is dependent on the earthquake scenario even for linear analysis based on the site-response analysis of several single-layer elastic soil sites that were subjected to a suite of seismic motions at rock sites. Scherbaum *et al.* [2011] and Bora *et al.* [2016] have further pointed out that the RSR may significantly differ from FSR particularly at short periods based on random vibration theory. Subsequently, Stafford *et al.* [2017] presented a theoretical explanation for why the two spectral ratios are different and why the RSR depends on the magnitude and distance of the earthquake scenario for linear analysis based on random vibration theory. Nearly all the aforementioned researches are based on theoretical analysis using random vibration theory or one-dimensional wave propagation theory.

Moreover, many studies have discussed the relationship between response and Fourier spectra. Zola [n.d.] introduced the basic relationship between the two spectra and their respective characteristics. Sutherland [1968] further explored their relationship by introducing a new concept of the residual shock spectrum. Udwadia and Trifunac [1973a,b] have discussed the relationship by developing another concept of the damped Fourier spectrum. Udwadia and Trifunac [1973b, 1974] have also discussed this problem using the extreme value statistics of oscillator response. Montejo and Vidot-Vega [2017] have developed an equation for connecting the Fourier amplitude spectrum with the acceleration response spectrum. Other studies have also investigated the relationship between the response spectrum with the power spectral density and time history. Sundararajan [1980]; Pfaffinger [1983], Park [1995], and Lanham *et al.* [2013] have developed methods for generating target power spectral density that is consistent with a response spectrum. Shin and Song [2016] and Li and Wang [2016] have proposed methods for generating a time history from a given response spectrum. However, the relationship between RSR and FSR was not discussed, which was also not the objective of these studies.

This study aims to statistically compare RSR and FSR using the actual ground motions recorded at natural nearby soil and rock sites. The rest of the paper is organized as follows. First, the nearby soil and rock sites as well as ground-motion records utilized in this study are detailed in Secs. 2 and 3, respectively. Then, by analyzing the seismic motions recorded at nearby soil and rock sites in Japan, the relationship between the two spectral ratios and the dependence of the RSR–FSR relationship on earthquake scenario and oscillator damping are investigated, in Sec. 4. Finally, the conclusions are presented in Sec. 5.

## 2. Nearby Soil and Rock Sites

In this study, RSR and FSR are calculated using ground-surface motions at nearby soil and rock sites instead of surface and borehole motions of a single site, although both are available in the Strong-motion Seismograph Networks (K-NET, KiK-net) of Japan [NIED, 1995]. The reasons are as follows:

- (1) Site effects are often estimated using the spectral ratio of surface recordings at nearby soil and rock sites, which is called the standard spectral ratio (SSR) [Héloïse *et al.*, 2012]. SSR was initially proposed by Borcherdt [1970] and has been widely used in numerous studies [Borcherdt, 1994; Dobry *et al.*, 2000; Zhao *et al.*, 2009; Zhao and Zhang, 2010].
- (2) The exploration of SSR has more practical engineering significance. Because in most seismic codes [International Conference of Building Officials, 1997; Ministry of Land, Infrastructure and Transport, 2000; ICC, 2012], spectral values are defined on a surface bedrock and site effects are characterized as SSR; therefore, the design spectrum on a soil site can be directly constructed by the product of the surface bedrock spectrum and SSR [Borcherdt, 1994; Dobry *et al.*, 2000].
- (3) Different from the surface bedrock, in the borehole station, both incident waves coming up from below and reflected waves going back from the surface are recorded. The spectral ratio of surface and borehole recordings can be affected not only by the amplification of surface soils but also by the interference of incident and reflected waves in the borehole station [Lee *et al.*, 2003]. Although borehole recordings can be approximately transformed to corresponding surface motions by analytical methods, this will complicate the calculation and increase the error.

It is generally considered that the spectral ratio of recordings at nearby soil and rock sites can reflect the effect of the soil site on the ground motion. To clarify this point, an illustration from a previous study of Avilés and Pérez-Rocha [2012] is used and shown in Fig. 1. This figure shows the relationship of the nearby soil and rock sites. The bedrock is considered to spread widely and beneath the soil site. In this study, the soil and rock sites are selected as closely as possible to meet this assumption. In this context, the bedrock and soil motions can be considered as input and output motions of the soil site, respectively. If we compute the Fourier spectral ratio of

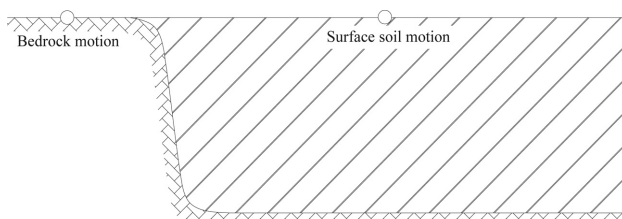


Fig. 1. Simplified reference model to explain the standard spectral ratio.

recordings at the soil and rock sites, the transfer function of the soil site can be obtained. The transfer function represents the soil amplification effect on the ground motion, and its peaks correspond to periods of the soil site. Therefore, the spectral ratio of recordings at nearby soil and rock sites can reflect soil amplification effect on the ground motion.

To systematically compare RSR and FSR, as many nearby soil and rock sites as possible are selected from the K-NET, KiK-net of Japan. The soil and rock sites are selected that have surface-layer shear wave velocities below and greater than 400 m/s, respectively, to meet the definition in the Japanese Seismic Design Code [Ministry of Land, Infrastructure and Transport, 2000]. In addition, to reduce the path effect on the spectral ratios, the soil sites are selected to be as close as possible to the rock site. Moreover, nearby soil and rock sites are selected that have sufficient strong-motion records for statistical analysis. A total of 10 pairs of nearby soil and rock sites satisfy the above conditions. Among the selected 10 pairs of soil and rock sites, the farthest distance from the rock to soil sites is 4.16 km, and the shortest distance is 0.01 km. The surface-layer shear wave velocities of the selected soil and rock sites vary from 70 m/s to 260 m/s and from 440 m/s to 1800 m/s, respectively. The selected 10 pairs of nearby soil and rock sites are numbered from 1 to 10; information for each pair of soil and rock sites, including the station code,

Table 1. Information for the selected 10 pairs of nearby soil and rock sites.

| Station ID |        | Coordinates ( $^{\circ}$ ) |         | —             | Site conditions |                 |
|------------|--------|----------------------------|---------|---------------|-----------------|-----------------|
| Name       | Code   | Long.                      | Lat.    | Distance (km) | $S$ (m/s)       | $V_{S30}$ (m/s) |
| 1          | AOMH03 | 140.9896                   | 41.234  | 4.10          | 530             | 653.7           |
|            | AOM006 | 140.9972                   | 41.1976 |               | 100             | 264.8           |
| 2          | CHBH20 | 140.0997                   | 35.0882 | 3.04          | 1800            | 1909.1          |
|            | CHB020 | 140.1022                   | 35.1155 |               | 150             | 134.4           |
| 3          | ISKH04 | 136.7176                   | 37.1902 | 4.16          | 440             | 443.5           |
|            | ISK006 | 136.6897                   | 37.1602 |               | 260             | 344             |
| 4          | YMGH01 | 131.5618                   | 34.0494 | 3.22          | 1000            | 1387.7          |
|            | YMG013 | 131.5348                   | 34.031  |               | 70              | 185.4           |
| 5          | NGSH06 | 129.8625                   | 32.6999 | 4.15          | 900             | 1421.1          |
|            | NGS010 | 129.8763                   | 32.7353 |               | 150             | 371.6           |
| 6          | GIFH20 | 137.2531                   | 35.7991 | 0.84          | 460             | 809.9           |
|            | GIF010 | 137.245                    | 35.8029 |               | 150             | 440.9           |
| 7          | GIFH14 | 137.5174                   | 36.2493 | 0.01          | 440             | 627.4           |
|            | GIF004 | 137.5174                   | 36.2492 |               | 230             | 452.7           |
| 8          | ISKH07 | 136.6357                   | 36.515  | 3.07          | 440             | 440             |
|            | ISK010 | 136.6431                   | 36.5419 |               | 110             | 388.2           |
| 9          | SRCH10 | 142.0085                   | 42.993  | 0.03          | 480             | 1026.8          |
|            | HKD123 | 142.0085                   | 42.9933 |               | 110             | 627.1           |
| 10         | MIE014 | 136.1687                   | 34.0638 | 0.02          | 880             | 1009.4          |
|            | MIEH05 | 136.1689                   | 34.0637 |               | 170             | 590.1           |

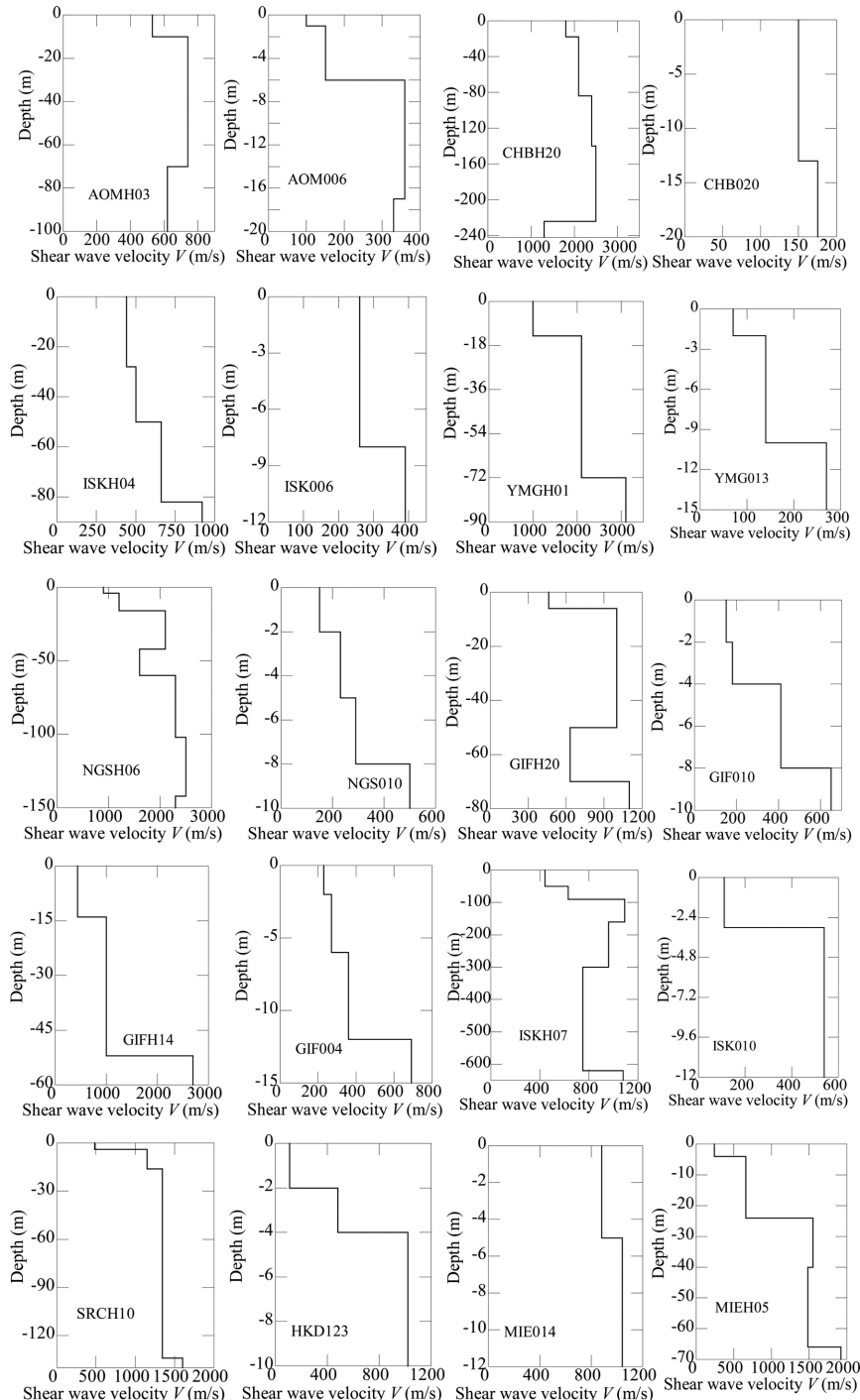


Fig. 2. Shear wave velocity profiles of the selected sites.

coordinates, distance from the rock to soil sites, surface-layer shear wave velocity,  $S$ , and average shear wave velocity in the upper 30 m,  $V_{S30}$ , are listed in Table 1. For each pair of soil and rock sites in the table, the upper line represents a rock site, and the lower line represents a soil site. In addition, shear wave velocity profiles of all the selected sites are presented in Fig. 2.

### 3. Ground-Motion Database

To systematically compare RSR and FSR, it is also necessary to select a large number of strong motions recorded on the 10 pairs of nearby soil and rock sites. To reduce the source effects on the spectral ratios, the ground motions from the same earthquakes that are simultaneously recorded at both the rock and nearby soil sites are selected. In addition, to control the signal-to-noise ratio and reduce the effect of noise, ground motions are selected that have peak accelerations above 5 gal. Moreover, to reduce the path effect on the spectral ratios, ground motions are selected that have epicentral distances that are more than 10 times the distance between the rock and nearby soil sites and less than 300 km. Finally, 510 ground-motion records from 232 earthquakes are selected from the K-NET, KiK-net. Each ground-motion record has two components: NS and EW. Thus, there are a total of 1020 earthquake time histories used in this study. Figure 3 shows the distributions of magnitudes,  $M_j$ , and epicentral distances of the used earthquakes. Here the magnitude,  $M_j$ , represents the Japan Meteorological Agency magnitude. The earthquakes have a wide range of magnitudes and epicentral distances. Because ground motions with a small magnitude can barely be recorded at a large epicentral distance, only few such records are obtained. Generally, the selected ground-motion records are with reasonably balanced distributions with respect to magnitude and epicentral distance.

In addition, all the selected ground-motion records are consistently processed. A baseline adjustment is applied to all records to remove long-period noise, and a

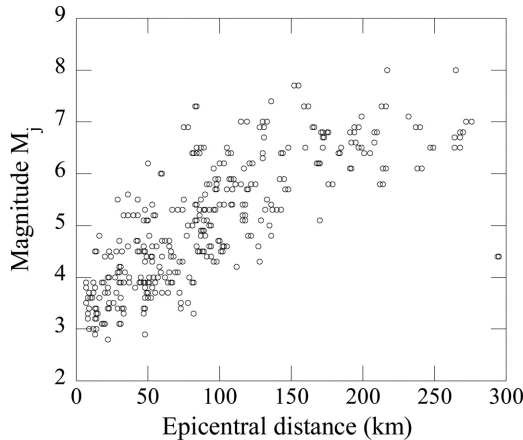


Fig. 3. Distributions of magnitudes and epicentral distances of the selected earthquakes.

low-pass filter with a corner frequency equaling 10 Hz is used to eliminate low-period noise. Because the corner frequency is 10 Hz for all the records, spectral ratios at periods larger than 0.1 s should not be severely affected by the low-pass filter.

## 4. Results of the Statistical Study

### 4.1. Comparison between the average RSR and FSR

To compare the RSR and FSR, the response spectra and Fourier spectra of all selected ground-motion records are computed. For the response spectra calculation, a 5% oscillator damping ratio is adopted. The Fourier amplitudes are smoothed using the Parzen window function with a bandwidth of 0.3. Then, the geometric means of the two components in EW and NS directions for each seismic record are calculated. Finally, the RSR and FSR are obtained as the quotients of the spectra for the soil sites compared with those for the rock sites. The comparisons of the average RSR and FSR for the 10 pairs of nearby soil and rock sites are shown in Fig. 4. Because the corner frequency of the low-pass filter is set to 10 Hz, and the upper bound period considered in seismic engineering is generally not above 10 s, this study focuses on the period band from 0.1 s to 10 s.

It is observed that the average RSR and FSR have similar overall shapes, and the maximum values of the two spectral ratios occur at approximately the same period, when the spectral ratios have obvious peaks. The spectral ratios for the five pairs of sites shown in the left column of Fig. 4 have obvious peaks, whereas those for the other five pairs show no obvious peaks. For the cases with no obvious peaks, the two spectral ratios have nearly the same values; however, for those with obvious peaks, the two spectral ratios can be obviously different. The difference between the two spectral ratios is most significant around the main spectral peak. At longer oscillator periods, the two spectral ratios are similar. RSR varies more smoothly with the oscillator period than FSR. Scherbaum *et al.* [2011], Bora *et al.* [2016], and Stafford *et al.* [2017] found that the two spectral ratios are very different over a very short period and can be similar at long oscillator periods based on random vibration theory. Their conclusions are basically consistent with the results observed above. However, because a low-pass filter is used to cut off the short-period noise, comparison over a very short period cannot be conducted in this study.

To explore the reason why no obvious peaks are observed, shear wave velocity profiles of the five pairs of soil and rock sites are analyzed. As presented in Fig. 2, although the surface-layer shear wave velocities of the five soil sites are below 400 m/s, the soft layers are very thin. The thicknesses of the soft layers that have a shear wave velocity below 400 m/s are only 4 m for GIF010, 12 m for GIF004, 3 m for ISK010, 2 m for HKD123, and 4 m for HIEH05. This leads that the site's fundamental period may be smaller than 0.1 s and could not be observed in the period of 0.1–10 s. Because these sites are the actual sites in Japan, structures may be built on such sites. Therefore, exploring their site effects is equally important for engineering.

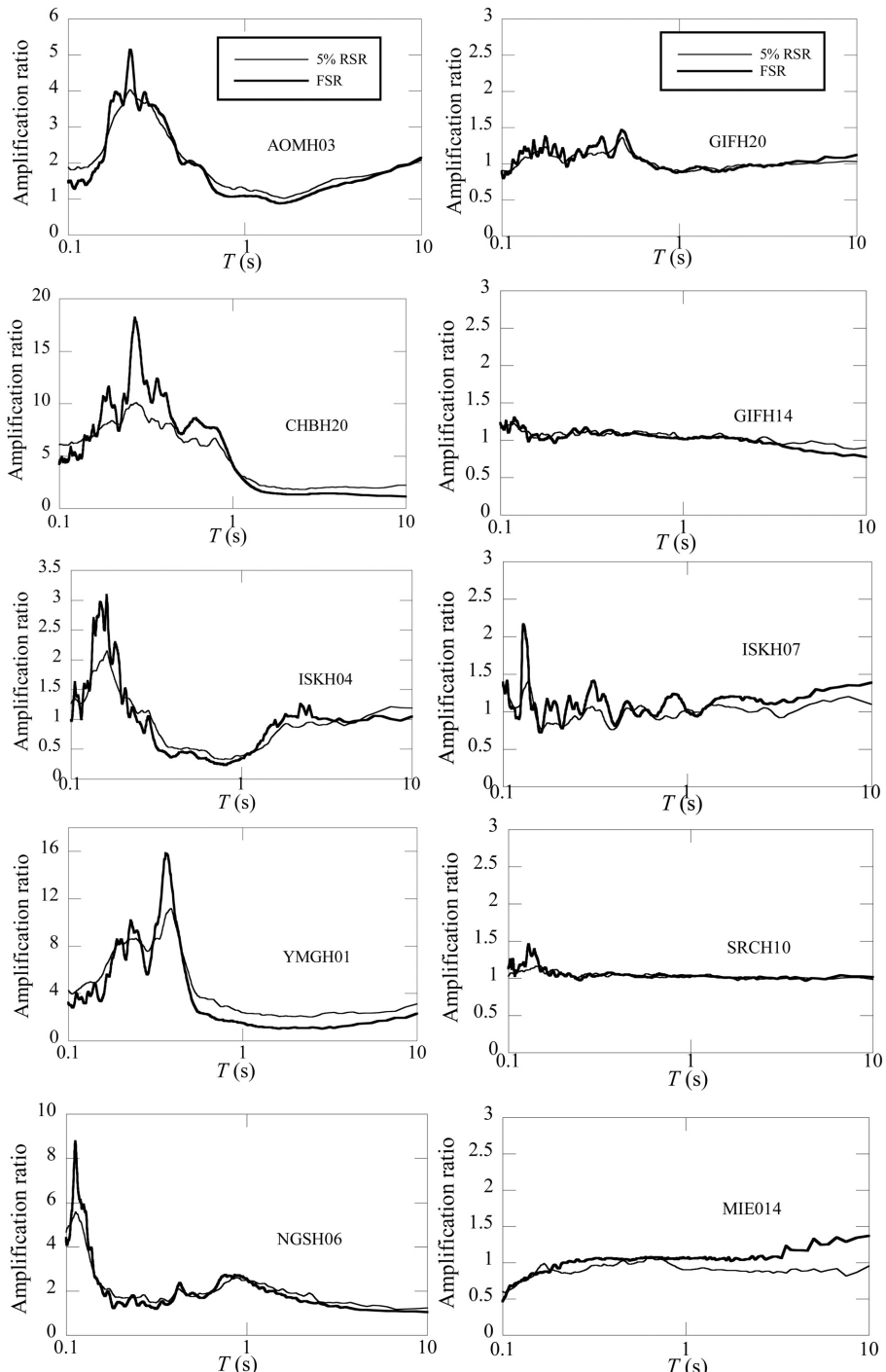


Fig. 4. Comparisons of the average RSR and FSR for the 10 pairs of soil and rock sites.

As amplification ratios of such sites are generally smaller than others in Fig. 4, their ground-motion intensity may be relatively smaller. However, when low structures, e.g. one- or two-story structures, with short natural periods are built on such sites, sufficient attention should be paid to avoid the occurrence of resonance.

#### 4.2. Effect of input rock motion

To investigate the dependence of the RSR–FSR relationship on the earthquake scenario, the selected ground motions in the previous section are classified into three groups according to magnitude and epicentral distance, as listed in Table 2. Figure 5 shows the number of earthquake records in each group. Groups 1–3 represent seismic motions with a small magnitude and short distance, seismic motions with a large magnitude and short distance, and seismic motions with a large magnitude and long distance, respectively. Therefore, by comparing the results from groups 1–3, the effects of magnitude and epicentral distance can be investigated.

The RSRs and FSRs belonging to the same group for each pair of soil and rock sites are averaged, respectively. Then, the average values of 5% damped RSR and FSR for each group are compared. Figure 6 shows the comparisons for the five pairs of soil and rock sites, in which the RSRs and FSRs have obvious peaks, whereas Fig. 7 shows the comparisons for the other five pairs of soil and rock sites, in which the RSRs and FSRs have no obvious peaks. The results of some groups for some sites are

Table 2. Classification of selected accelerograms.

| Group | Magnitude | Epicentral distance (km) |
|-------|-----------|--------------------------|
| 1     | 2.8–5     | 7–150                    |
| 2     | 5.1–8     | 7–150                    |
| 3     | 5.1–8     | 151–300                  |

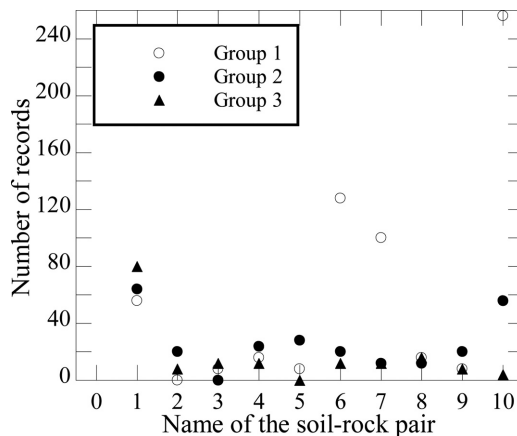


Fig. 5. Number of records in each group.

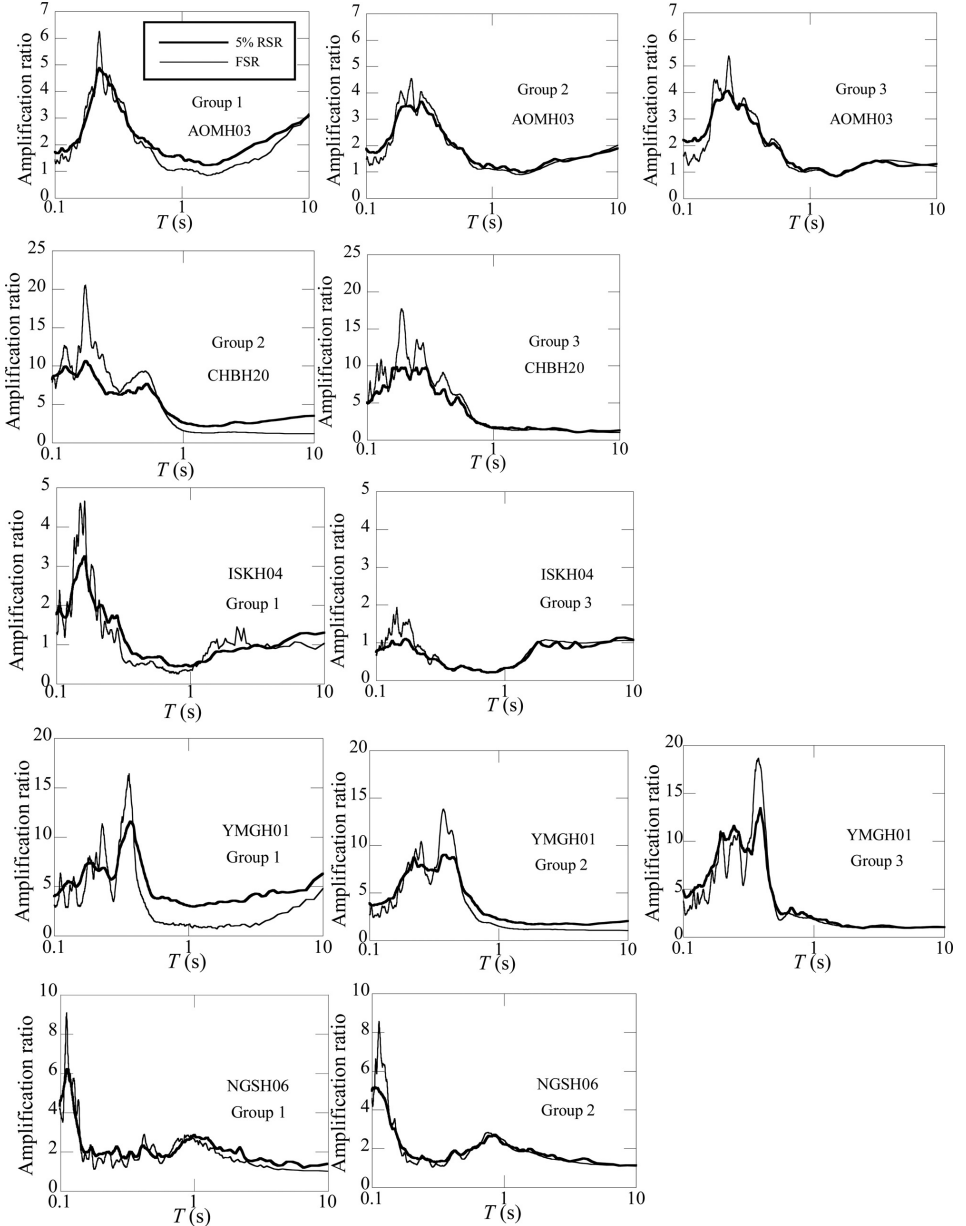


Fig. 6. Comparison of RSRs and FSRs for each group of the five pairs of soil and rock sites, in which the spectral ratios show obvious peaks.

lacking, as shown in Fig. 6. This is because among the selected seismic motion data described in the previous section, there are no data belonging to these groups for these sites, although seismic records are selected as much as possible. By comparing the results of groups 1–3 in Fig. 6, it is found that at periods longer than the site's

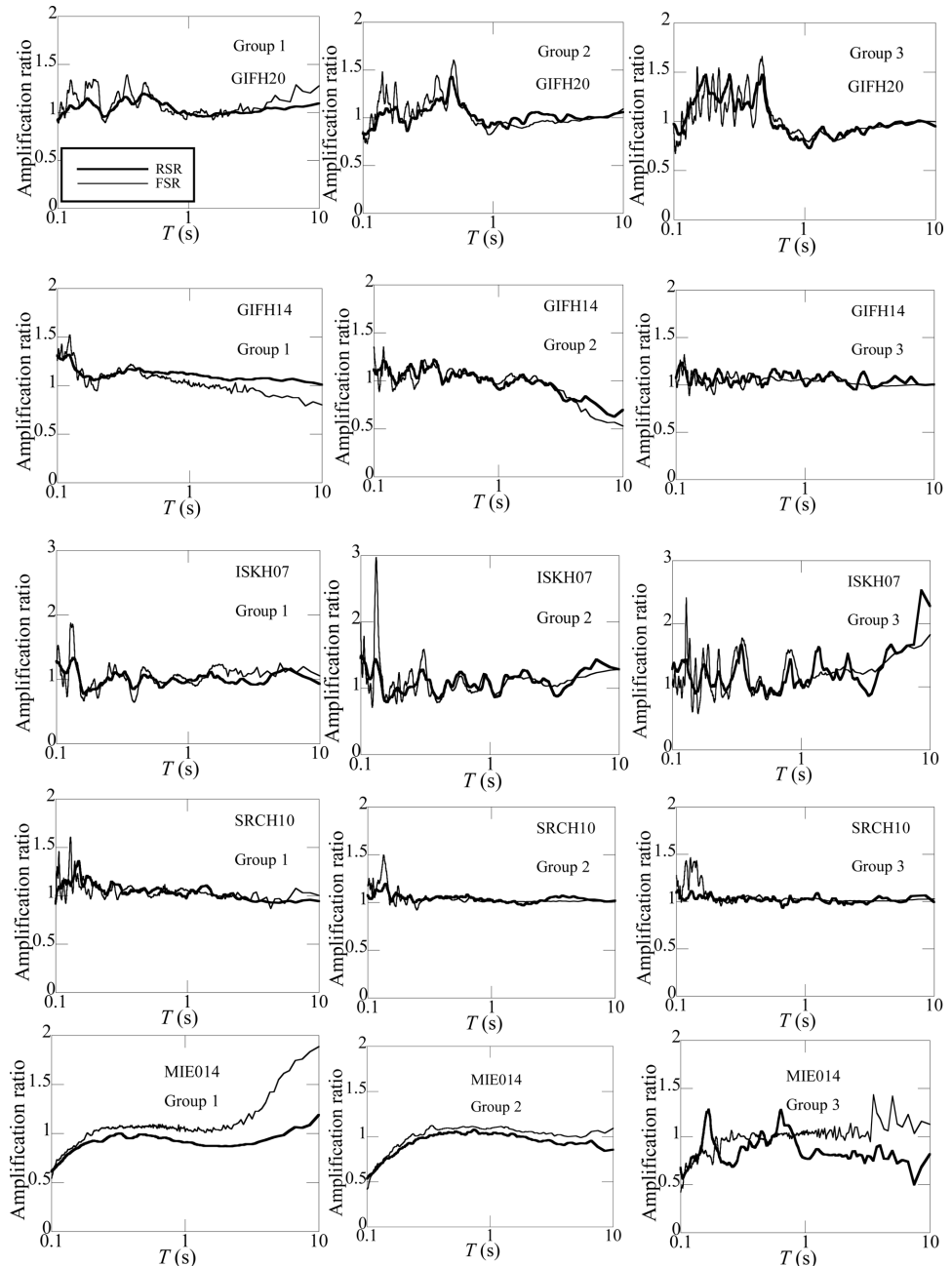


Fig. 7. Comparison of RSRs and FSRs for each group of the five pairs of soil and rock sites, in which the spectral ratios have no obvious peaks.

fundamental period  $T_f$ , the difference between the RSR and FSR decreases as the magnitude and epicentral distance increase. A representative ratio of RSR to FSR at 2 s is used to quantify the agreement between the RSR and FSR at periods longer than the site's fundamental period  $T_f$ . The RSRs and FSRs at 2 s and the ratios of RSR to FSR at 2 s are provided in Table 3. It is observed that all the 2-s ratios approach unity with increasing group number, which supports the conclusion that the difference between RSR and FSR decreases as the magnitude and epicentral distance increase. Stafford *et al.* [2017] found that the difference between RSR and FSR at very short periods increases with an increase in magnitude and distance, which is not clearly observed in Fig. 6. This may be due to the use of the low-pass filter, which cuts off the short-period noise ( $< 0.1$  s) and makes comparison over the short period impossible.

In addition, the comparison of each group in Fig. 6 shows that the overall shapes of RSR and FSR are very similar, and their maximum peaks occur at approximately the same period with FSR consistently exceeding the RSR. The maximum peak values of RSR and FSR and the corresponding periods for each group are shown in Table 3. The ratio of the maximum peak values and ratio of the periods between RSR and FSR for each group are calculated and shown in the table. The period ratios for each group are near unity, and the maximum peak value ratios for each group are smaller than unity. It is also noted that amplification ratios in groups 2 and 3 of the CHBH20 station are higher than those of other stations. This occurs because the contrast between shear wave velocities of the soil and rock sites is very large, as can be seen in Fig. 2.

Moreover, the results of the five pairs of soil and rock sites in which the spectral ratios have no obvious peaks, are analyzed. For these sites, the RSRs are nearly identical to the FSRs and approximately equal to unity for each group. The dependence of the RSR–FSR relationship on the magnitude and epicentral distance is not that obvious as for the results in Fig. 6. Nevertheless, for long periods, the difference between RSR and FSR tends to decrease as the magnitude and epicentral distance increase. However, for the sites MIE014 and ISKH07, the shapes of RSR and FSR for group 3 are more jagged, and the difference between RSR and FSR in group 3 is larger compared with those for groups 1 and 2. This is perhaps because that there is only one earthquake for group 3 for the two sites, and the spectral ratios of the single earthquake cannot be smoothed by the average as for other groups that have many earthquakes.

It is known that FSR purely reflects site effects and is independent of the earthquake scenario for linear analysis. However, Fig. 6 shows that not only the RSR but also the FSR varies with the magnitude and epicentral distance. This occurs because the soil behaves nonlinearly when subjected to strong earthquake motions, or when the incident angles of seismic waves are different. As the analysis is based on real seismic motions recorded on natural sites, these effects can hardly be removed.

In addition, the peak ground acceleration (PGA) threshold for sites to demonstrate nonlinearity is investigated. It is observed from the YMGH01 station in Fig. 8

Table 3. Results for the five pairs of soil and rock sites for different groups, in which the spectral ratios have obvious peaks.

| Name | Group | RSR $T_f$ | FSR $T_f$ | Period ratio | RSR <sub>max</sub> | FSR <sub>max</sub> | RSR <sub>max</sub> /FSR <sub>max</sub> | RSR (2 s) | FSR (2 s) | RSR (2 s)/FSR (2 s) |
|------|-------|-----------|-----------|--------------|--------------------|--------------------|----------------------------------------|-----------|-----------|---------------------|
| 1    | 1     | 0.22      | 0.22      | 1            | 4.88               | 6.25               | 0.78                                   | 1.32      | 0.96      | 1.38                |
|      | 2     | 0.27      | 0.23      | 1.21         | 3.66               | 4.55               | 0.81                                   | 1.04      | 0.97      | 1.07                |
|      | 3     | 0.23      | 0.23      | 0.99         | 4.06               | 5.38               | 0.75                                   | 1.06      | 1.01      | 1.05                |
| 2    | 2     | 0.27      | 0.27      | 1            | 10.64              | 20.53              | 0.52                                   | 2.19      | 1.32      | 1.67                |
|      | 3     | 0.26      | 0.28      | 0.92         | 9.83               | 17.69              | 0.56                                   | 1.59      | 1.39      | 1.14                |
| 3    | 1     | 0.16      | 0.16      | 1            | 3.25               | 4.66               | 0.70                                   | 0.83      | 1.03      | 0.80                |
|      | 2     | 0.17      | 0.14      | 1.18         | 1.10               | 1.93               | 0.57                                   | 0.92      | 1.07      | 0.86                |
|      | 3     | 0.37      | 0.36      | 1.02         | 11.56              | 16.43              | 0.70                                   | 3.42      | 1.16      | 2.94                |
| 4    | 1     | 0.39      | 0.38      | 1.03         | 9.01               | 13.84              | 0.65                                   | 1.70      | 1.18      | 1.44                |
|      | 3     | 0.39      | 0.38      | 1.03         | 13.43              | 18.67              | 0.72                                   | 1.06      | 1.01      | 1.05                |
| 5    | 1     | 0.11      | 0.11      | 1.01         | 6.16               | 9.04               | 0.68                                   | 1.92      | 1.46      | 1.32                |
|      | 2     | 0.11      | 0.11      | 0.94         | 5.16               | 8.56               | 0.60                                   | 1.70      | 1.56      | 1.09                |

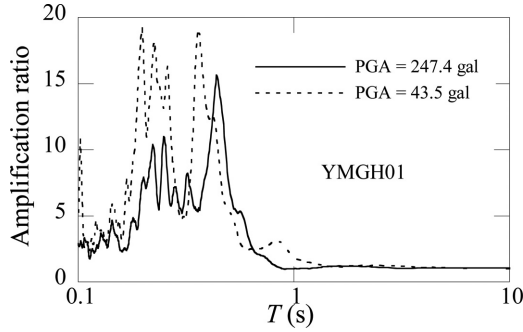


Fig. 8. Variation of the amplification ratio with PGA.

that, when PGA is as large as 247.4 gal, the soil site shows clear nonlinear characteristics, the site fundamental period becomes longer, and amplification ratios at short periods decrease. The PGA threshold for soil nonlinearity is not that clear for other four stations in Fig. 6. The reason may be that PGAs of selected motions in these stations are not that large (<150 gal), although the earthquake motions recorded at these stations are selected as much as possible.

#### 4.3. Effect of the oscillator damping ratio

As the RSR is dependent on the oscillator damping ratio, the RSR–FSR relationship should also be dependent on the oscillator damping ratio. To investigate the effect of the oscillator damping ratio, three values of the oscillator damping ratio, 1%, 5%, and 10%, are considered in the calculation of RSR. The averaged RSRs with different damping ratios are compared with FSRs for each pair of soil and rock sites, as presented in Fig. 9.

As presented in Fig. 9, the RSR is dependent on the oscillator damping ratio. The RSR values approach those of FSR upon decreasing the oscillator damping, and this trend is most prominent near the maximum peak. Three representative values of the RSR–FSR ratio at 0.1 s, the maximum peak, and 2 s are selected to further investigate the dependence of the RSR–FSR relationship on the oscillator damping ratio. The RSRs and FSRs at 0.1 s and 2 s as well as the calculated ratios of RSR to FSR for these periods are provided in Table 4. Most of these ratios approach unity with decreasing oscillator damping ratio, which supports the idea that the RSR values approach those of FSR with decreasing oscillator damping ratio.

For the five pairs of soil rock sites, in which the spectral ratios have no obvious peaks, the RSRs are almost identical to the FSRs and approximately equal to unity for all oscillator damping ratios. Nevertheless, the RSRs vary slightly and approach the FSRs with decreasing oscillator damping.

In addition, as presented in Fig. 9, for all oscillator damping ratios, the two spectral ratios have very similar overall shapes, and the shape of the RSR is relatively flatter. The maximum peaks for RSR and FSR occur at approximately the same

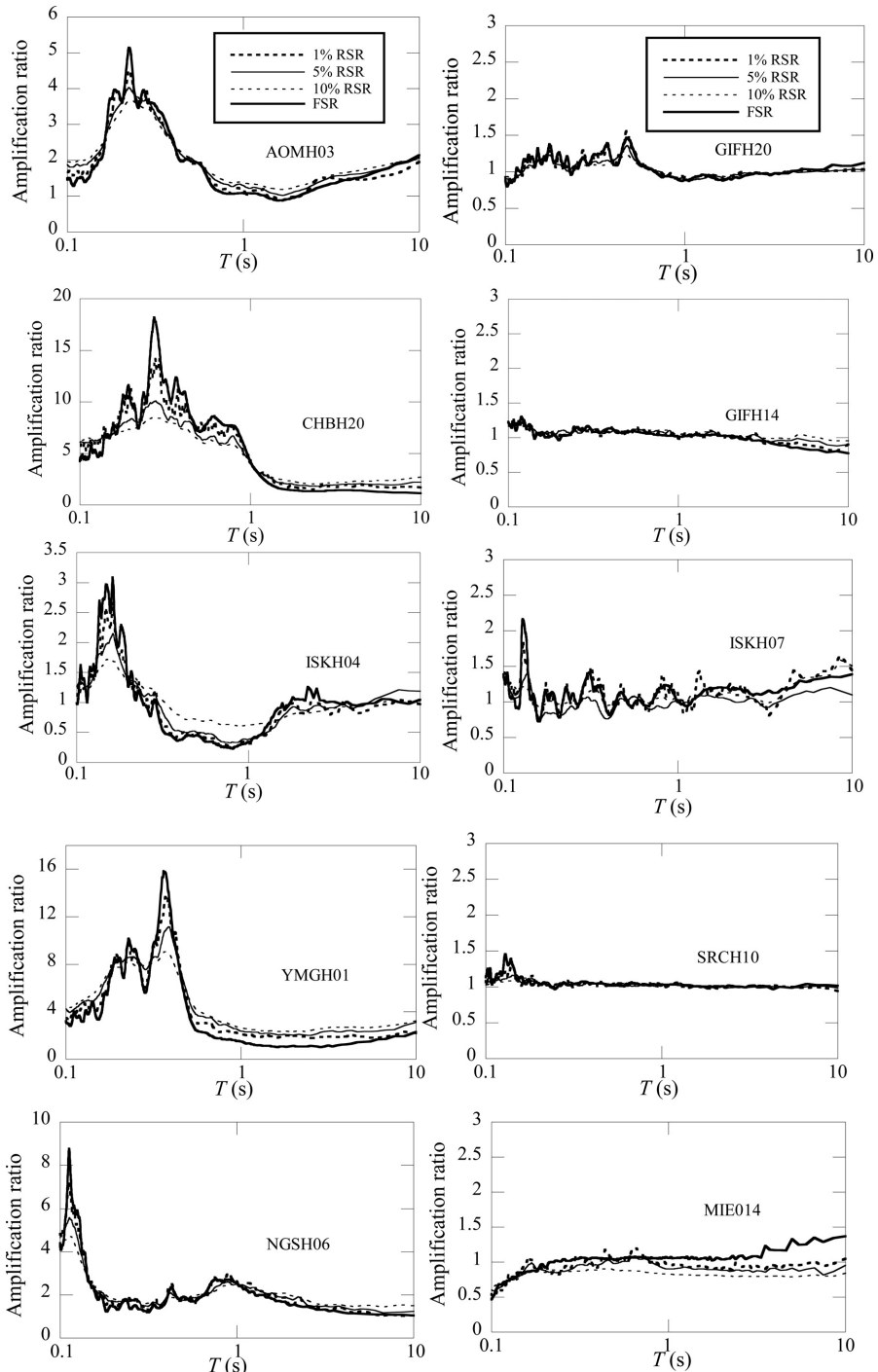


Fig. 9. Comparisons of FSR and RSR for different oscillator damping ratios.

Table 4. Results for the five pairs of soil and rock sites for different damping ratios, in which the spectral ratios have obvious peaks.

| Name | $T_f$ (s) | $T_f$ (s) ratio | Peak value | Peak-value ratio | Value ratio |          | Value ratio<br>at 2 s |
|------|-----------|-----------------|------------|------------------|-------------|----------|-----------------------|
|      |           |                 |            |                  | at 0.1 s    | at 0.1 s |                       |
| 1    | 1% RSR    | 0.22            | 1          | 4.52             | 0.88        | 1.67     | 1.13                  |
|      | 5% RSR    | 0.22            | 1          | 4.03             | 0.78        | 1.88     | 1.27                  |
|      | 10% RSR   | 0.23            | 1.05       | 3.67             | 0.71        | 1.98     | 1.34                  |
|      | FSR       | 0.22            | —          | 5.14             | —           | 1.48     | —                     |
|      |           |                 |            |                  |             |          | 0.98                  |
| 2    | 1% RSR    | 0.28            | 1.04       | 14.26            | 0.78        | 5.62     | 1.32                  |
|      | 5% RSR    | 0.28            | 1.04       | 10.09            | 0.55        | 6.10     | 1.44                  |
|      | 10% RSR   | 0.27            | 1          | 8.48             | 0.47        | 6.17     | 1.45                  |
|      | FSR       | 0.27            | —          | 18.19            | —           | 4.25     | —                     |
|      |           |                 |            |                  |             |          | 1.35                  |
| 3    | 1% RSR    | 0.16            | 1          | 2.67             | 0.87        | 1.06     | 1.07                  |
|      | 5% RSR    | 0.16            | 1          | 2.15             | 0.70        | 1.27     | 1.28                  |
|      | 10% RSR   | 0.15            | 0.94       | 1.72             | 0.56        | 1.27     | 1.28                  |
|      | FSR       | 0.16            | —          | 3.08             | —           | 0.99     | —                     |
|      |           |                 |            |                  |             |          | 1.05                  |
| 4    | 1% RSR    | 0.37            | 1.03       | 13.66            | 0.86        | 3.71     | 1.17                  |
|      | 5% RSR    | 0.39            | 1.08       | 11.17            | 0.71        | 4.25     | 1.34                  |
|      | 10% RSR   | 0.37            | 1.03       | 9.07             | 0.57        | 4.32     | 1.36                  |
|      | FSR       | 0.36            | —          | 15.83            | —           | 3.18     | —                     |
|      |           |                 |            |                  |             |          | 1.12                  |
| 5    | 1% RSR    | 0.11            | 1          | 7.19             | 0.82        | 4.78     | 1.10                  |
|      | 5% RSR    | 0.11            | 1          | 5.58             | 0.64        | 4.68     | 1.08                  |
|      | 10% RSR   | 0.12            | 1.09       | 4.70             | 0.54        | 4.43     | 1.02                  |
|      | FSR       | 0.11            | —          | 8.77             | —           | 4.33     | —                     |
|      |           |                 |            |                  |             |          | 1.51                  |

period with the FSR peak consistently exceeding the RSR peak. To further investigate the relationship between the maximum peaks of RSR and FSR, their maximum peak values and the corresponding periods are obtained and listed in Table 4. Then, the ratio of the maximum peak values and the ratio of the periods between the two spectral ratios are computed and are listed in the table. All the period ratios are near unity, and all the maximum peak ratios are smaller than unity. This indicates that the maximum peak values for the two spectral ratios occur at nearly the same period with that for FSR consistently exceeding that for RSR for any damping condition.

## 5. Conclusions

This study statistically investigates the relationship between the RSR and FSR by analyzing a lot of seismic ground motions recorded on 10 pairs of nearby soil and rock sites in Japan. The following systemic relationships between the two spectral ratios are found:

- (1) The shape of RSR is very similar to that of FSR. When the two spectral ratios have obvious peaks, the maximum peak values of RSR and FSR occur at approximately the same period with that of FSR consistently exceeding that of RSR.
- (2) The relationship between RSR and FSR is dependent on the earthquake scenario and ultimately the magnitude and epicentral distance. For long periods, the difference between RSR and FSR decreases with increasing magnitude and epicentral distance. This trend is particularly prominent for spectral ratios that have obvious peaks.
- (3) The relationship between RSR and FSR is dependent on the oscillator damping ratio, and RSRs generally approach the FSRs with decreasing oscillator damping ratio. This trend is particularly prominent for spectral ratios that have obvious peaks.

## Acknowledgments

The study is partially supported by the National Natural Science Foundation of China (Grant No. 51738001). The support is gratefully acknowledged.

## References

- Avilés, J. and Pérez-Rocha, L. E. [2012] “Revisions to code provisions for site effects and soil-structure interaction in Mexico,” in *Earthquake Research and Analysis — New Frontiers in Seismology*, ed. Sebastiano D’Amico (IntechOpen, Rijeka), pp. 237–254.
- Bora, S. S., Scherbaum, F., Kuehn, N. and Stafford, P. J. [2016] “On the relationship between Fourier and response spectra: Implications for the adjustment of empirical ground-motion prediction equations (GMPEs),” *Bull. Seismol. Soc. Am.* **106**(3), 1235–1253.

- Borcherdt, R. D. [1970] "Effect on local geology on ground motion near San Francisco Bay," *Bull. Seismol. Soc. Am.* **60**(1), 29–61.
- Borcherdt, R. D. [1994] "Estimates of site-dependent response spectra for design (methodology and justification)," *Earthq. Spectra* **10**, 617–653.
- Dobry, R., Borcherdt, R. D., Crouse, C. B., Idriss, I. M., Joyner, W. B., Martin, G. R., Power, M. S., Rinne, E. E. and Seed, R. B. [2000] "New site coefficients and site classification system used in recent building seismic code provisions," *Earthq. Spectra* **16**(1), 41–67.
- Héloïse, C., Bard, P.-Y. and Rodriguez-Marek, A. [2012] "Site effect assessment using KiK-net data: Part 1: A simple correction procedure for surface/downhole spectral ratios," *Bull. Earthq. Eng.* **10**(2), 421–448.
- Ibrahim, R., Si, H., Koketsu, K. and Miyake, H. [2014] "Empirical spectral acceleration amplification in the Iwate–Miyagi and Niigata regions, Japan, inferred by a spectral ratio method using ground-motion prediction equations," *Bull. Seismol. Soc. Am.* **104**(3), 1410–1429.
- International Code Council (ICC) [2012] *2012 International Building Code* (International Code Council, Inc., Country Club Hills, IL).
- International Conference of Building Officials [1997] *1997 Uniform Building Code*, Vol. 1 (International Conference of Building Officials, Whittier, CA).
- Lanham, K., Khoncarly, M. and Todorovski, L. [2013] "Alternative method for converting seismic response spectra to target power spectral density," *Proc. 22nd Conf. Structural Mechanics in Reactor Technology*, pp. 1–11.
- Lee, W. H. K., Kanamori, H., Jennings, P. C. and Kisslinger, C. [2003] "Site effects on strong ground motions," in *International Handbook of Earthquake & Engineering Seismology: Part B*, H Kawase (ed.) (Academic Press, San Diego, CA), pp. 1013–1014.
- Li, X. J., Liu, L., Wang, Y. S. and Yu, T. [2010] "Analysis of horizontal strong-motion attenuation in the great 2008 Wenchuan earthquake," *Bull. Seismol. Soc. Am.* **100**(5B), 2440–2449.
- Li, Y. and Wang, G. [2016] "Simulation and generation of spectrum-compatible ground motions based on wavelet packet method," *Soil Dyn. Earthq. Eng.* **87**, 44–51.
- Midorikawa, M., Okawa, I., Iiba, M. and Teshigawara, M. [2003] "Performance-based seismic design code for buildings in Japan," *Earthq. Eng. Eng. Seismol.* **4**(1), 15–25.
- Ministry of Land, Infrastructure and Transport [2000] "Japanese Seismic Design Code: Technical standard for structural calculation of response and limit strength of buildings, 2000," Notification No. 1457-2000 (in Japanese).
- Miura, K., Koyamada, K. and Iiba, M. [2001] "Response spectrum method for evaluating nonlinear amplification of surface strata," *J. Struct. Construct. Eng. (Trans. AIJ)* **539**, 57–62 (in Japanese).
- Montejo, L. A. and Vidot-Vega, A. L. [2017] "An empirical relationship between Fourier and response spectra using spectrum-compatible times series," *Earthq. Spectra* **33**(1), 179–199.
- National Research Institute for Earth Science and Disaster Resilience (NIED) [1995] "Strong-motion Seismograph Networks (K-NET, KIK-net)," Available at: <http://www.kyoshin.bosai.go.jp/kyoshin/> (accessed on August 8, 2019).
- Park, Y. J. [1995] "New conversion method from response spectrum to PSD functions," *J. Eng. Mech., ASCE* **121**(12), 1391–1392.
- Pfaffinger, D. D. [1983] "Calculation of power spectra from response spectra," *J. Eng. Mech., ASCE* **109**(1), 357–372.
- Scherbaum, F., Seif, S. and Kuehn, M. [2011] "On the relationship between Fourier and response spectra consequences for the adjustment of empirical ground-motion prediction

- equations for regional differences,” *Proc. American Geophysical Union, Fall Meeting 2011.*
- Shin, G. and Song, O. [2016] “A time-domain method to generate artificial time history from a given reference response spectrum,” *Nucl. Eng. Technol.* **48**(3), 831–839.
- Stafford, P. J., Rodriguez-Marek, A., Edwards, B., Kruiver, P. and Bommer, J. J. [2017] “Scenario dependence of linear site effect factors for short-period response spectral ordinates,” *Bull. Seismol. Soc. Am.* **107**(6), 2859–2872.
- Sundararajan, C. [1980] “An iterative method for the generation of seismic power spectral density functions,” *Nucl. Eng. Des.* **61**(1), 13–23.
- Sutherland, L. C. [1968] “Fourier spectra and shock spectra — A generalized approach for simple undamped systems,” Research Staff Technical Memorandum No. 67-4, WYLE Laboratories, Research Division, Huntsville Facility.
- Udwadia, F. E. and Trifunac, M. D. [1973a] “Damped Fourier spectrum and response spectra,” *Bull. Seismol. Soc. Am.* **63**(5), 1775–1783.
- Udwadia, F. E. and Trifunac, M. D. [1973b] “The Fourier transform, response spectra and their relationship through the statistics of oscillator response,” CALTECH Report No. EERL 73-01, Earthquake Engineering Research Laboratory, California Institute of Technology, Pasadena, CA.
- Udwadia, F. E. and Trifunac, M. D. [1974] “Characterization of response spectra through the statistics of oscillator response,” *Bull. Seismol. Soc. Am.* **64**(1), 205–219.
- Zhang, H. Z. and Zhao, Y. G. [2018] “A simple approach for estimating the first resonance peak of layered soil profiles,” *J. Earthq. Tsunami* **12**(03), 1850005.
- Zhang, H. Z. and Zhao, Y. G. [2019] “A simple approach for estimating the fundamental mode shape of layered soil profiles,” *J. Earthq. Tsunami* **13**(01), 1950003.
- Zhang, H. Z., Saito, T. and Zhao, Y. G. [2017] “Simple calculation method of seismic motion amplification ratio corresponding to fundamental period,” *J. Struct. Construct. Eng. (Trans. AJ)* **82**(734), 597–604 (in Japanese).
- Zhao, J. X. and Zhang, J. [2010] “Side-effect of using response spectral amplification ratios for soft soil sites — Earthquake source-type dependent amplification ratios,” *Soil Dyn. Earthq. Eng.* **30**(4), 258–269.
- Zhao, J. X., Zhang, J. and Kojiro, I. [2009] “Side effect of using response spectral amplification ratios for soil sites-variability and earthquake-magnitude and source-distance dependent amplification ratios for soil sites,” *Soil Dyn. Earthq. Eng.* **29**(9), 1262–1273.
- Zola, M. [n.d.] “The relationship between shock response spectrum and fast Fourier transform,” Background material, ISMES, LMC, Italy. Available at: <https://www.osti.gov/etdeweb/servlets/purl/20327252> (accessed on 2020 September 20).